Nanophotonic Phased Array for Visible Light Image Projection

Manan Raval[1], Ami Yaacobi[1], Daniel Coleman[2], Nicholas M. Fahrenkopf[2], Christopher Baiocco[2], Gerald Leake[2], Thomas N. Adam[2], Douglas Coolbaugh[2], and Michael R. Watts[1]
[1]Research Laboratory of Electronics, Massachusetts Institute of Technology, Cambridge, MA, USA 02139
[2] Colleges of Nanoscale Science and Engineering, SUNY Polytechnic Institute, Albany, NY, USA 12203
mraval@mit.edu

***Abstract*— We demonstrate the first large-scale integrated nanophotonic phased array for visible wavelengths in a silicon nitride platform. The array consists of 32×32 optical antenna elements designed to project complex intensity patterns in the far field at a wavelength of λ = 635 nm.**

Keywords—Photonic integrated circuits, Phased arrays, Displays

I. Introduction

Silicon-based nanophotonic phased arrays have been widely investigated for developing fully functional chip-scale systems for applications including light detection and ranging (LIDAR) and free-space optical communications [1,2]. The high index contrast and compatibility with state-of-the-art Complementary Metal-Oxide Semiconductor (CMOS) fabrication technology afforded by silicon have enabled large-scale high density photonic integrated circuits (PICs) for the development of nanophotonic phased arrays [3]. Integrated optical phased arrays demonstrated to date have operated primarily in the C- (1530-1565 nm) and L-bands (1565-1625 nm), where silicon provides low loss transmission. However, applications such as autostereoscopic image projection for 3D displays [4] and neuronal targeting for optogenetics [5] would benefit greatly from nanophotonic phased arrays operating in the visible spectrum, which are to-date unexplored in an integrated photonics platform.

In this work, we demonstrate the first visible light phased array implemented in an integrated photonics platform. The phased array is fabricated in silicon nitride and is designed for an operating wavelength of 635 nm. While it is transparent to visible light, silicon nitride is also CMOS compatible and provides relatively high index contrast with respect to silicon dioxide cladding, thereby enabling dense large-scale PICs in the visible spectrum [6]. These advantages were leveraged for the fabrication of a phased array comprised of 1024 nanoantennas with 4-µm emitter pitch in a state-of-the-art CMOS foundry. Phase information was passively encoded into individual antennas for projecting complex far-field intensity patterns.

II. Fabrication and Results

Fig. 1 shows a schematic of the 32×32 passive silicon nitride phased array. An external 635-nm light source is edge coupled from a single-mode fiber to a silicon nitride bus waveguide, from which the signal is evenly distributed to 32 row waveguides via a series of directional couplers by varying their length along the bus waveguide. Light in each row waveguide is then evenly coupled to 32 optical emitters along the waveguide in a similar manner. Delivery of an equal amount of optical power to each emitter ensures a uniform emission profile in the near field, as seen in Fig. 2(a). Each unit cell (Fig. 1 inset) is comprised of a directional coupler and a short waveguide section terminated with a compact upward emitting grating. A slight offset is applied between the directional coupler waveguide and the curved waveguide in the unit cell to compensate for mode mismatch between the two waveguide regions in order to minimize bend loss.

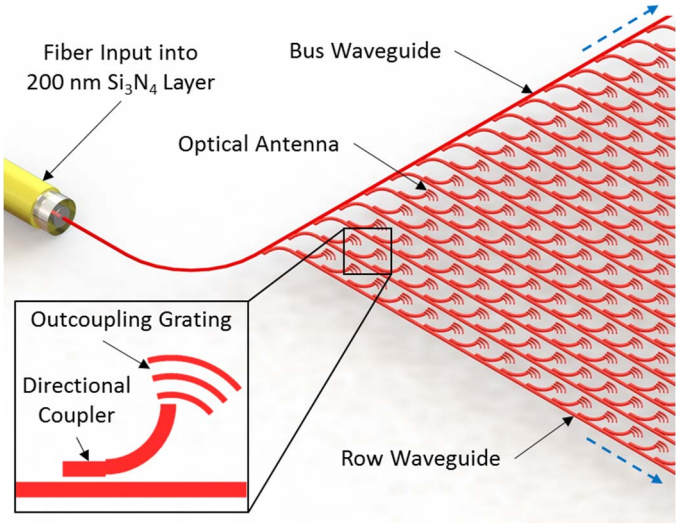

Fig. 1. Schematic of the large scale silicon nitride optical phased array for 635 nm emission. Inset: schematic of single phased array unit cell.

In this passive configuration, the phase of the emitted signal of each emitter is set by varying the relative location of the unit cell along its corresponding row waveguide with respect to its default position according to a 4 µm pitch grid, as expressed in Fig. 2(b). The unit cell may be displaced from its default location by a distance equivalent to $\pm\lambda/2$ with respect to the waveguide mode to achieve full 2π phase tuning. Since this displacement is subwavelength and of significantly lower magnitude than the

emitter pitch, the noise induced in the far field by the spatial offsets of unit cells is negligible.

The necessary near-field phase distribution for generating a specific far-field intensity pattern can be calculated using the Gerchberg-Saxton (GS) algorithm [7]. Fig. 2(c) shows the necessary near-field phase distribution of a 32×32 phased array for generating an azimuthal perspective image of a pyramid, shown in Fig. 2(d), in the far field using this algorithm. Shading is applied to one of the faces of the target image of the pyramid to test the ability to generate varied intensity images in the far field while tuning only phase in the near field. The finite emitter count and the lack of control over emitter emission amplitude prevent the iterative GS algorithm from achieving a near-field phase distribution with a corresponding far-field pattern that converges completely to the target far field, but a very close approximation, shown in Fig. 2(e), can still be achieved.

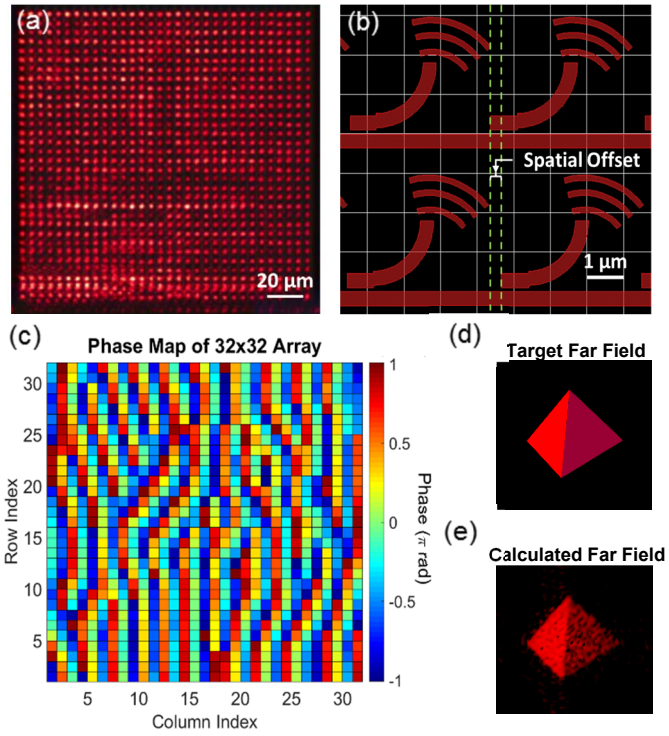

Fig. 2. (a) Captured image of the near-field emission of 32×32 phased array. (b) Example of unit cell displacement for passive phase encoding. (c) Phase distribution of 32×32 phased array for generating a perspective image of a pyramid in the far field as calculated by the GS algorithm. (d) Target far-field image. (e) Resulting zeroth order far-field image from GS algorithm.

The presented structure was fabricated in a state-of-the-art CMOS foundry on a 300-mm wafer with a 200-nm silicon nitride layer using 193-nm optical immersion lithography. The simulated and measured far fields of two silicon nitride phased arrays encoded with the phases necessary for projecting two different azimuthal perspectives of a pyramid are shown in Fig. 3. Higher order images are seen in the far field because the emitter pitch is larger than a wavelength. The uniform near-field emission profile as well as good agreement between the simulated and measured far-field intensity patterns of the phased array demonstrate the robustness of the CMOS fabrication process utilized in this work.

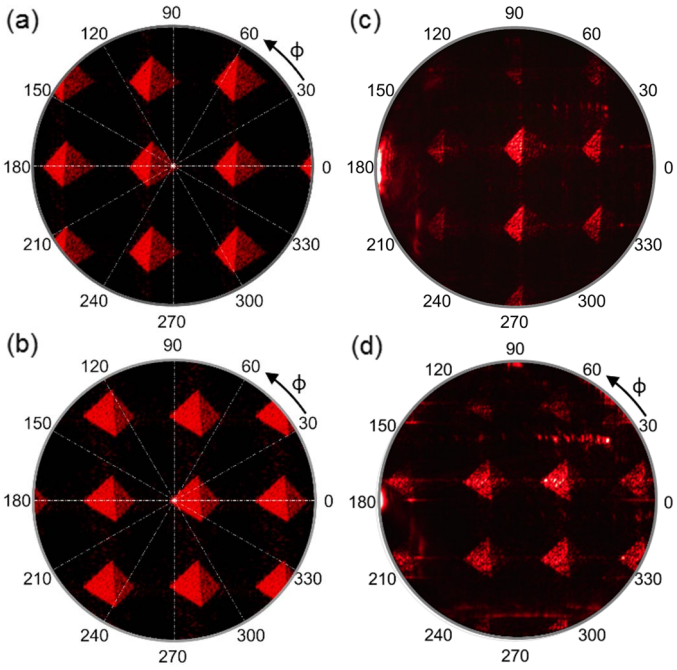

Fig. 3. (a,b) Simulated far-field radiation patterns for two different azimuthal perspective images of a pyramid. (c,d) Corresponding measured far-field radiation patterns generated by 32×32 emitter phased arrays.

III. Conclusion

We demonstrate the first visible light phased array for arbitrary far-field image projection implemented in a silicon nitride integrated photonic platform. Active electro-optic tuning of emitter phases may be incorporated in the future by integrating nematic liquid crystals onto the photonic chip or fabricating the PIC in a III-V material system. Further development of phased arrays in the visible spectrum will enable applications such as high-resolution augmented reality systems and glass-free autostereoscopic and holographic 3D displays.

This work was supported by the Defense Advanced Research Projects Agency (DARPA) E-PHI program under Grant No. HR0011-12-2-0007 and a National Defense Science & Engineering Graduate (NDSEG) Fellowship to M. Raval.

References

[1] J. C. Hulme et al., "Fully integrated hybrid silicon two dimensional beam scanner," Opt. Express, vol. 23, pp. 5861-5874, 2015.

[2] A. Yaacobi, J. Sun, M. Moresco, G. Leake, D. Coolbaugh, and M. R. Watts, "Integrated phased array for wide-angle beam steering," Opt. Lett., vol. 39, pp. 4575-4578, 2014.

[3] J. Sun, E. Timurdogan, A. Yaacobi, E. S. Hosseini, and M. R. Watts, "Large-scale nanophotonic phased array," Nature, vol. 493, no. 7431, pp.195-199, 2013.

[4] J. Hong, Y. Kim, H. J. Choi, J. Hahn, J. H. Park, H. Kim, and B. Lee, "Three-dimensional display technologies of recent interest: principles, status, and issues [Invited]." Appl. Optics, vol. 50, no. 34, 2011.

[5] F. Zhang et al., "Optogenetic interrogation of neural circuits: technology for probing mammalian brain structures." Nat. Protoc., vol. 5, issue 3, pp. 439-456, 2010.

[6] S. Romero-García, F. Merget, F. Zhong, H. Finkelstein, and J. Witzens, "Silicon nitride CMOS-compatible platform for integrated photonics applications at visible wavelengths," Opt. Express, vol. 21, pp. 14036-14046, 2013.

[7] J. R. Fienup, "Reconstruction of an object from the modulus of its Fourier transform," Opt. Lett., vol.3, no.1, pp. 2729, 1978.